Correlation of high numbers of intratumoral FOXP3+ regulatory T cells with improved survival in germinal center-like diffuse large B-cell lymphoma, follicular lymphoma and classical Hodgkin's lymphoma

Alexandar Tzankov,[1] Cecile Meier,[1] Petra Hirschmann,[1] Philip Went,[2] Stefano A. Pileri,[3] and Stephan Dirnhofer[1]

[1]Institute of Pathology, University Hospital Basel, Switzerland; [2]Institute of Pathology, Triemli Hospital, Zurich, Switzerland; [3]Chair of Pathology and Unit of Hematopathology, Institute of Hematology and Clinical Oncology "L. and A. Seràgnoli", University of Bologna, Italy

Acknowledgments: we thank D. Wolf, (Department of Hematology and Oncology, University Hospital Innsbruck, Austria) and M.G. Uguccioni, (Institute for Research in Biomedicine, Bellinzona, Switzerland) for critically reading the manuscript, and M.K. Occhipinti-Bender for editorial assistance.

Manuscript received July 13, 2007. Manuscript accepted November 28, 2007.

Correspondence: Alexandar Tzankov, MD, Department of Pathology, University Hospital Basel, Schoenbeinstr. 40, CH-4031 Basel, Switzerland. E-mail: atzankov@uhbs.ch

The online version of this article contains a supplemental appendix.

ABSTRACT

Background
The tumor microenvironment is important for the behavior of cancer. We assessed the distribution and biological significance of FOXP3+ regulatory T-cells (Treg) in lymphomas.

Design and Methods
The absolute number of intratumoral FOXP3+ cells was immunohistochemically studied on lymphoma tissue microarrays from 1019 cases of different types of lymphomas and correlated to phenotypic and clinical parameters in uni- and multivariate models. Receiver operating characteristic - curves were used to determine prognostic cut-off values of FOXP3+ cell density.

Results
Of the 1019 cases, 926 (91%) were evaluable. FOXP3+ cell density varied between the lymphoma entities, and was highest in follicular lymphoma. An increased number of tumor-infiltrating FOXP3+ cells over the receiver operating characteristic-determined cut-offs positively influenced both disease-specific and failure-free survival in follicular lymphoma (p=0.053) and disease-specific survival in germinal center-like diffuse large B-cell lymphoma (p=0.051) and overall and failure-free survival in classical Hodgkin's lymphoma (p=0.004), but had a negative prognostic effect in non-germinal center diffuse large B-cell lymphoma (p=0.059). In a Cox regression model, considering stage and age, the amount of FOXP3+ cells was of independent prognostic significance for failure-free survival in classical Hodgkin's lymphoma and of borderline significance for overall survival in classical Hodgkin's lymphoma and disease-specific survival in germinal center-like and non-germinal center diffuse large B-cell lymphoma.

Conclusions
FOXP3+ cells represent important lymphoma/host microenvironment modulators. Assessment of FOXP3+ cell density can contribute to the prediction of outcome in diffuse large B-cell lymphoma, fallicular lymphoma and classical Hodgkin's lymphoma.

Key words: lymphoma, Treg, FOXP3, tissue microarray, receiver operating characteristic curves

Citation: Tzankov A, Meier C, Hirschmann P, Went P, Pileri SA, and Dirnhofer S. Correlation of high numbers of intratumoral FOXP3+ regulatory T-cells with improved survival in germinal center-like diffuse large B-cell lymphoma, follicular lymphoma and classical Hodgkin's lymphoma. Haematologica 2008 Feb; 93(2):193-200. DOI:10.3324/haematol.11702

©2008 Ferrata Storti Foundation. This is an open-access paper.

©Ferrata Storti Foundation

Introduction

The tumor microenvironment is an important factor in the development and progression of cancer.[1,2] A subset of regulatory T-cells (Treg) in the tumor microenvironment, characterized by a $CD4^+CD25^+$ phenotype, has become the focus of interest, given the critical role of these cells in the modification of immune responses, particularly suppression of tumor-associated antigen-reactive lymphocytes.[1,3] Identification of the *forkhead* transcription factor FOXP3 as a master regulator of Treg development enabled more precise definition of this cell population.[4,5] It has been convincingly shown that FOXP3 is required for Treg suppressor activity, amplifying and fixing Treg molecular features, generating and maintaining their phenotype,[6] and that *FOXP3* gene transfer to $CD4^+$ cells is sufficient to induce transplantation tolerance.[7]

Recent evidence suggests that the cellular composition of the tumor microenvironment, particularly the quantity of tumor-infiltrating Treg, can significantly modify the clinical outcome in hematologic malignancies, particularly in follicular lymphomas (FL) and classical Hodgkin's lymphomas (cHL).[8-11] Importantly, the transforming lymphomagenesis events in both FL and cHL probably occur during the so-called germinal center (GC) reaction,[12,13] which is the most important step in B-cell maturation during T-cell dependent antigen responses.[14] The so-called follicular helper T cells (T_{FH}) are thought to play a considerable role in inducing somatic hypermutation and immunoglobulin (Ig) class switching in B cells undergoing a GC reaction.[15-18] It has been shown that Treg potently suppress T_{FH} and T_{FH}-mediated B-cell functions such as Ig production and B-cell survival.[19,20] Moreover, $FOXP3^+$ Treg can directly suppress and even kill B cells.[21,22]

The importance of tumor-infiltrating $FOXP3^+$ cells in lymphomas has been addressed in only a few studies thus far.[9-11,23-27] To further characterize the distribution and correlate the quantity of tumor-infiltrating $FOXP3^+$ cells to phenotypic and clinical parameters in lymphomas, we performed a tissue microarray (TMA) analysis on previously validated TMA, encompassing 1019 cases, applying receiver operator characteristics (ROC)-based methods to determine prognostic cut-off levels of $FOXP3^+$ cell density.

Design and Methods

Samples

Mature B- and T-cell lymphomas and cHL cases (n=1019) diagnosed between 1974 and 2001 and reclassified according to current criteria[28] were collected from the archives of the Institutes of Pathology at the Universities of Basel, Innsbruck and Bologna. Paraffin blocks were selected based on availability and preservation. Clinical and follow-up data (Table 1) were obtained from chart reviews. Tissue and clinical data were retrieved according to the regulations of the local institutional review boards and data protection laws. Details on treatment regimens and definitions of response, relapse and treatment failures are given in the online *Supplementary Data*.

©Ferrata Storti Foundation

Table 1. Characteristics of the patients for whom tissue microarray were constructed. The number of cases with known International Prognostic Index scores in DLBCL and the presence of B-symptoms in cHL cases are indicated in brackets.

Lymphoma	N	%	Stage				Age (mean±SD)	M:F	N follow-up	Overall survival		
			I (IPI 0-1)	II (IPI 2)	III (IPI 3)	IV/known (IPI 4-5 or BS)				Mean months	Median months	Relative 5-year %
SLL/CLL	85	12					66±11	2.1	63	94	105	74
Mantle cell lymphoma	19	2	0	3	0	8/11	64±14	5	15	37	22	19
Primary DLBCL	270	36	28 (67)	50 (30)	34 (32)	49/161 (23/153)	63±16	1.2	207	85	42	52
Secondary DLBCL	31	4	1	4	3	10/17	63±12	1.3	27	49	16	36
Follicular lymphoma G1-3	86	12	4	22	5	28/59	57±15	0.6	82	126	not reached	83
Burkitt's lymphoma	6	0.8	0	1	0	0/1	20±7	1	0			
MZL of MALT	73	10	30	15	0	0/45	62±14	1.3	42	181	219	88
MZL + DLBCL	58	8					65±16	1.2	44	77	71	54
PMBCL	51	7					29±13	0.2	0			
PTCL, NOS	28	4	1	0	2	4/7	66±16	1.5	16	54	16	36
Angioimmunoblastic [T-cell lymphoma	28	4	0	0	7	8/15	68±14	1.2	18	37	22	35
Anaplastic large [cell lymphoma	4	0.5					35±27	1	1			
Total B-/T-cell lymphomas	**739**								**515**			
cHL, nodular sclerosis	156	56	6	38	15	22/81 (28)	34±16	1	84	244	269	86
cHL, mixed cellularity	93	33	10	15	7	6/38 (19)	44±21	2	49	163	130	75
cHL, lymphocyte rich	11	4	0	1	3	0/4 (2)	42±18	1.2	6	232	not reached	75
cHL, lymphocyte depleted	7	2	0	1	1	0/2 (0)	482±16	1.3	4	200	192	75
cHL, unclassifiable	13	5	0	5	4	0/9 (5)	44±20	1.6	9	225	not reached	100
Total cHL	**280**								**152**			

IPI, International Prognostic Index; BS, B-symptoms; SLL/CLL, small lymphocytic lymphoma/chronic lymphocytic leukemia; G1-3, grades 1-3; MZL, marginal zone lymphoma; PMBCL, primary mediastinal B-cell lymphoma; PTCL, NOS, peripheral T-cell lymphoma, not otherwise specified

Tissue microarray construction

The tissue microarray (TMA) were constructed and validated as described elsewhere[29-35] (see *Supplementary Data*). In cases of FL, neoplastic GC were sampled for arraying.

Morphometrical analysis

The total number of cells and, in cases of cHL, of Hodgkin and Reed-Sternberg cells (HRSC) on the array spots was counted on hematoxylin and eosin-stained slides and, in cases of cHL, on CD30 stained slides at 200 magnification. All morphometric results were mathematically referred to 1 mm^2. In cases of FL, the results were extrapolated to 1 mm^2 of GC tissue.

Immunohistochemistry

TMA slides were processed for FOXP3 staining on an automated immunostainer (Nexes, Ventana, Tucson, AZ, USA). Heat-induced (microwave oven) antigen retrieval in EDTA buffer (pH 8.0) for 30 minutes at 100°C was performed. The streptavidin-biotin-peroxidase detection technique with diaminobenzidine as chromogen was applied. The primary monoclonal anti-FOXP3 antibody (clone 22510 from Abcam, Cambridge, UK) was diluted 1:200 in a 1% solution of bovine serum albumin in phosphate-buffered saline (pH 7.4) and the slides were incubated for 32 minutes at 37°C. For double-stains see *Supplementary Data*. Other relevant primary antibodies considered, their dilutions and antigen retrieval conditions are detailed in our previous publications.[29,31-33,35] Because intensity varies between cases due to different tissue preservation, only the absolute count of positively staining cells, and not the staining intensity, was considered. The FOXP3 staining was validated on 14 lymph nodes and tonsils. To assess the agreement of the staining results for FOXP3 between conventional- and TMA slides, a direct comparison was performed in 35 arrayed cases [12 diffuse large B-cell lymphomas (DLBCL), 7 FL, 5 small lymphocytic lymphomas/chronic lymphocytic leukemias (SLL/CLL), 2 angioimmunoblastic T-cell lymphomas (AILT), 4 anaplastic large cell lymphomas (ALCL), and 5 cHL]. Applying Hans' algorithm[36] with cut-off values for markers determined by ROC (i.e. 15% for CD10, 30% for bcl-6 and 65% for MUM1; see *Statistics*), DLBCL cases were classified as phenotypically GC-like, non-GC DLBCL or unclassifiable.

Statistics

Statistical analysis including data description was done using the Statistical Package of Social Sciences 14.0 software (Chicago, IL, USA). The agreement between immunohistochemical results from the TMA and conventional full-tissue sections was assessed using the κ statistics, a κ-value of ≥ 0.75 implying excellent agreement. The Pearson χ^2 statistic was used to analyze relationships between the markers and the clinical variables. Analysis of variables (ANOVA) was applied to assess mean differences between groups. The prognostic performance of these variables and determination of optimal cut-off values of continuous variables was established by ROC-curves plotting sensitivity versus 1-specificity. The optimal cut-off point was calculated using Youden's index (Y), where Y=sensitivity+specificity–1, since this method can be applied when there is no particular requirement on sensitivity and/or specificity.[37] The results from the ROC analysis were considered in every disease entity for overall, disease-specific and failure-free survival. These survival rates were then analyzed by the Kaplan-Meier method applying the cut-off values calculated by the ROC/Y. Survival results for which the ROC or the Kaplan-Meier method indicated statistical significance ($p<0.05$) or borderline significance ($p<0.1$) were further considered. The impact of markers that seemed to be of significant or borderline prognostic significance in univariate analyses determined by multivariate analysis done using a Cox regression model.

©Ferrata Storti Foundation

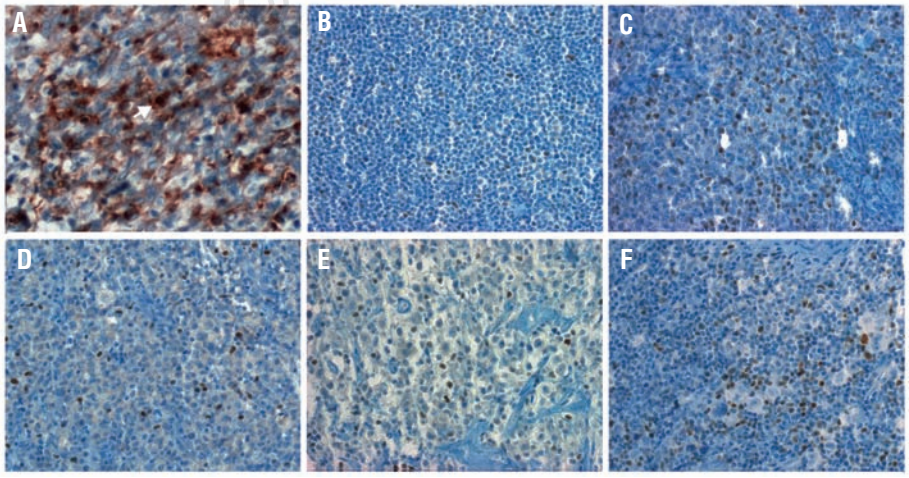

Figure 1. A. Co-expression of CD4 (membranous/submembranous, red) and FOXP3 (nuclear, brown) cells in tonsillar T-lymphocytes. Note the co-localization of staining signals in 14 cells (one highlighted with an arrow) as well as functioning internal negative controls - many $CD4^+/FOXP3^-$ T cells. Immunoperoxidase staining, ×400 magnification. **B.** Isolated $FOXP3^+$ cells in small lymphocytic lymphoma. Immunoperoxidase stain, ×400 magnification. **C.** Numerous $FOXP3^+$ cells in follicular lymphoma, grade 3. Immunoperoxidase stain, ×400 magnification. **D.** $FOXP3^+$ cells in diffuse large B-cell lymphoma. Immunoperoxidase stain, ×400 magnification. **E.** $FOXP3^+$ cells in angioimmunoblastic T-cell lymphoma. Immunoperoxidase stain, ×400 magnification. **F.** $FOXP3^+$ cells in Hodgkin's lymphoma. Note Hodgkin and Reed-Sternberg cells as well as small groups of FOXP3-positive cells. Immunoperoxidase stain, ×400 magnification.

Results

Patients and determination of phenotypic GC-like DLCBL

All the relevant clinical characteristics of the patients are shown in Table 1. For additional life status data see *Supplementary Data*. Applying the modified Hans' algorithm (see *Statistics*), DLBCL cases were classified as phenotypically GC-like (n=81), non-GC DLBCL (n=98) or, due to lacking data on single markers from the decision tree, unclassifiable DLBCL (n=91).

FOXP3 expression and TMA validation

In normal tissues, FOXP3 was moderately expressed in tonsillar and nodal lymphocyte nuclei with a distribution accentuated in the subepithelial and marginal zones of the tonsils (mean 35±17 FOXP3$^+$ cells/mm^2 marginal zone tissue), paracortical areas (mean 15±9 FOXP3$^+$ cells/mm^2 paracortical tissue) and follicles of both tonsils and lymph nodes (mean 18±11 FOXP3$^+$ cells/mm^2 GC tissue). Unequivocal co-expression of FOXP3 and CD4 or CD25, was detectable on double-stained slides, while expression of FOXP3 on CD4 or CD25-negative cells was not observed (Figure 1A). Comparison of results of conventional lymphoma slides and TMA showed good concordance (κ=0.87), which was lower in FL (κ=0.79) and cHL (κ=0.80), and higher in SLL/CLL (κ=0.92), ALCL (κ=0.95) and DLBCL (κ=0.94).

Distribution of FOXP3$^+$ tumor-infiltrating lymphocytes

FOXP3$^+$ cells could be assessed on TMA for 677 (92%) B- and T-cell lymphomas and 249 (89%) cHL (Table 2). The analysis failure rate was within the expected range for TMA.[30] FOXP3$^+$ cell count and density varied between the studied lymphoma entities from 0 to 882/mm^2 (mean 32/mm^2) and 0 to 48% (mean 1.6%) in B- and T-cell lymphomas and from 0 to 626/mm^2 (mean 42/mm^2) and 0 to 22% (mean 1.8%) in cHL, being higher in FL, AILT, nodular sclerosis cHL, primary mediastinal B-cell lymphomas (PMBCL) and peripheral T-cell lymphomas (PTCL) and lower in marginal zone lymphomas (MZL), mantle cell lymphomas (MCL) and lymphocyte-rich cHL (Figure 1 B-F). In cHL, FOXP3$^+$ cells were rarely in the direct proximity to HRSC. We did not detect FOXP3-expression on the atypical cells of PTCL and AILT or on any B-cell lymphoma cells and HRSC (Figure1 B-F). Despite *in vitro* data on the ability of the NPM/ALK oncoprotein to induce a Treg cell phenotype with expression of FOXP3 mRNA in ALCL,[38] we did not detect FOXP3 protein expression in the lymphoma nuclei of the four arrayed ALK$^+$ ALCL, although tumor-infiltrating FOXP3$^+$ small lymphocytes were present. All morphometric results are summarized in Table 2 and partially shown in Figure 1B-F.

Statistics

Correlations of FOXP3$^+$ cell quantity with infiltrating T cells and lymphoma transformation

There were specific associations between the numbers of FOXP3$^+$ cells/mm^2 and CD3$^+$ T cells in all phenotypic subtypes of primary DLBCL (p=0.001; correlation coefficient 0.343) and in FL (p=0.008; correlation coefficient 0.292), but

©Ferrata Storti Foundation

Table 2. Morphometric characteristics and FOXP3$^+$ cell density in arrayed B- and T-cell- and classical Hodgkin's lymphomas.

Lymphoma	*N. evaluable*	*%*	*FOXP3$^+$/mm^2*	*FOXP3$^+$ proportion*	*Cells/core=0.283 mm^2*	*Hodgkin's and Reed-Sternberg cells/core (mean±SD)*
SLL/CLL	84	99	21±26	0.4±0.8	2157±1164	
Mantle cell lymphoma	19	100	23±33	0.2±0.4	2730±933	
Primary DLBCL	248	92	27±34	2.1±6	912±676	
GC-like[36]	81		25±39	2.2±5.9	902±678	
non-GC[36]	98		28±44	1.8±5.1	863±661	
unclassifiable	91		27±41	2.4±5.8	892±666	
Secondary DLBCL	28	88	37±62	1.8±3.2	1075±812	
Follicular lymphoma G1-3	83	97	94±71	2.5±4.8	1729±1016	
Burkitt's lymphoma	6	100	6±4	0.4±0.7	730±317	
MZL of MALT	60	82	2±2	0.08±0.3	921±400	
MZL+DLBCL	47	81	2±2	0.1±00.4	482±153	
PMBCL	48	94	37±74	2.6±4.7	626±390	
PTCL, NOS	27	99	34±54	2.6±4.7	1317±1101	
Angioimmunoblastic	23	82	61±84	2.2±3.1	954±548	
[T-cell Lymphoma						
Anaplastic large	4	100	15±11	3.9±6.7	706±773	
[cell lymphoma						
p^{ANOVA}			<0.0001	<0.0001	<0.0001	
cHL, nodular sclerosis	138	86	49±71	2±3.1	1325±821	13±20
cHL, mixed cellularity	87	91	38±63	1.7±3.7	1074±700	8±12
cHL, lymphocyte rich	9	100	7±11	0.2±0.4	1724±635	5±7
cHL, lymphocyte depleted	5	71	33±29	1.9±2.8	604 ±20	28±47
cHL, unclassifiable	10	100	21±16	1.9±4	705±311	10±8
p^{ANOVA}						0.034

SLL/CLL, small lymphocytic lymphoma/chronic lymphocytic leukemia; G1-3, grades 1-3; MZL, marginal zone lymphoma; PMBCL, primary mediastinal B-cell lymphoma; PTCL, NOS, peripheral T-cell lymphoma, not otherwise specified

not with the number of CD4+ tumor-infiltrating lymphocytes. In cHL cases there was no correlation between the number of FOXP3+ cells/mm² and Epstein-Barr virus-status, but there was a weak correlation with the number of CD3+ T cells (p=0.045; correlation coefficient 0.138). Except for transformed DLBCL evolving from FL, which showed decreased amounts of FOXP3+ cells (33/mm²) compared to FL (94/mm², p=0.075), DLBCL evolving from SLL/CLL and MZL with a DLBCL-component showed no specific changes of FOXP3+ cell amounts compared to SLL/CLL and MZL. For additional data see *Supplementary Data*.

Setting the cut-off values for FOXP3+ cell quantity

ROC showed significant discriminatory power considering overall, disease-specific and failure-free survival rates for the number of tumor-infiltrating FOXP3+ cells in FL, DLBCL, CLL/SLL and cHL (Table 3). A typical ROC curve for the discriminatory power of the number of FOXP3+ cells is shown in Figure 2A. Comparison of the results linked to clinical end-points by the Kaplan-Meier method unequivocally showed the superior discriminating power of the cut-off levels calculated considering the ROC/Y compared to means, medians and quartile values (see *Supplementary Figure*).

Survival analysis associated with quantity of FOXP3+ cells

Overall, disease-specific and failure-free survival rates were analyzed by the Kaplan-Meier method applying cut-off values determined by the ROC/Y and primary dichotomized clinical characteristics. The absolute amount of tumor-infiltrating FOXP3+ cells was of significant prognostic importance for overall and disease-specific survival in DLBCL, disease-specific and failure-free survival in FL, and overall and failure-free survival in cHL (Figure 2B-F). A trend toward better overall survival was observed in AILT, with >40.4 FOXP3+ cells/mm² (p=0.191). All relevant results concerning the prognostic importance of tumor-infiltrating FOXP3+ cells are shown in Table 3 and Figure 2B-F. In a Cox regression model the amount of tumor-infiltrating FOXP3+ cells was of independent prognostic significance for failure-free survival in cHL and of borderline significance for overall survival in cHL and disease-specific survival in GC-like and non-GC DLBCL (Table 4), in DLBCL, in general, not being independent of the International Prognostic Index (*data not shown*).

Discussion

Our analyses extended results of previous studies on tumor-infiltrating FOXP3+ cells in lymphomas by taking advantage of validated lymphoma TMA with continuous referencing to 1 mm², application of commercially-available monoclonal antibodies in a large cohort (n=1019) of cases with distributions, except for SLL/CLL, similar to that expected in an average Middle European population,[39] and a ROC-curve based approach to calculate optimal cut-off-points for the prognostic evaluation of FOXP3+ cell numbers. The soundness of our analysis, the multiple previous validations of the TMA used[29-35] as well as the κ-values for the comparison of results from conventional lymphoma slides and TMA guarantee the reliability of the data obtained. We clearly demonstrated that the FOXP3+ cell density varies between different lymphoma types and that do lymphoma-infiltrating FOXP3+ cells may represent important lymphoma/host microenvironment-modulators, since increased amounts of these cells can positively influence survival in FL, GC-like DLBCL and cHL. Because neither CD3+ nor CD4+ tumor infiltrating lymphocytes correlated with prognosis, but only the amount of FOXP3+ cells, the latter obviously do not simply reflect the T-cell infiltration (see *last paragraph of the Discussion*).

Our FOXP3+ data are concordant with flow cytometry data from 24 B-cell lymphoma patients[25] showing that CD4+CD25+ cells represent 17% of the median amount of 19% (i.e. 3%) CD4+ cells in the lymphoma specimens. Nevertheless, our results are partially at variance with those of other immunohistochemical studies.[9,10,26] Some differences between our results and those of these studies could be attributed to different anti-FOXP3 antibodies and dilutions (undiluted, clone 236A/E7M,[9,10] 1:25 dilution, clone mAbcam 22510[26] and 1:200 dilution, clone mAbcam

Table 3. Determination of optimal cut-off levels considering overall survival, disease-specific survival and failure-free survival for FOXP3+ cell density applying receiver operating characteristic curves; the *p* values in the ROC-columns consider the discriminatory power of the suggested cut-off, the next two percent values correspond to the sensitivity and specificity of the test at the chosen cut-off value.

Entity	*FOXP3+ ROC^{OS}*	*OS^{K-M}*	*FOXP3+ ROC^{DSS}*	*DSS^{K-M}*	*FOXP3+ ROC^{FFS}*	*FFS^{K-M}*
GC-like DLBCL	4.5/mm² (p=0.115; 85/41%)	0.062	4.4/mm² (p=0.089; 67/58%)	0.051		
non-GC DLBCL			*6.1/mm² (p=0.066; 70/50%)*	*0.059*		
FL G1-3			88.6/mm² (p=0.107; 40/91%)	0.053	88.6/mm² (p=0.115; 40/91%)	0.05
SLL/CLL	8.8/mm² (p=0.150; 47/75%)	0.083				
cHL, all	27.2/mm² (p=0.029; 35/87%)	0.004			18.4/mm² (p=0.026; 45/82%)	0.004
cHL, nodular sclerosis					18.7/mm² (p=0.031; 50/88%)	0.003
cHL, mixed cellularity	3.5/mm² (p=0.062; 52/74%)	0.063			3.5/mm² (p=0.102; 54/71%)	0.051

The significance of FOXP3+ cell density considering OS, DSS and FFS was tested after dichotomization by the Kaplan-Meier (K-M) method. Factors in which values above the cut-off had adverse prognostic effects are shown in italics. ROC, receiver operating characteristic; OS, overall survival; DSS, disease-specific survival; FFS, failure-free survival

©Ferrata Storti Foundation

22510 [*our study*]). Importantly, the antibody clone 236A/E7M stained a notably larger population of cells than another anti-FOXP3 monoclonal antibody (14-5779, eBioscience, San Diego, CA, USA),[40] and validation experiments of the staining specificity of mAbcam 22510 used at 1:25 dilution were not reported.[26] In FL, in particular, differences could be related to our *a priori* arraying of cores from neoplastic GC for TMA construction and consideration of conventional slides by Carreras *et al.*[10] The peri- and interfollicular FOXP3$^+$ cells,[11] which are reportedly more numerous than those in the follicular compartment,[10] were not, therefore, included in our assessment. Nevertheless, the proportional decrease of FOXP3$^+$ cells in FL and transformed DLBCL evolving from FL observed by us was 2.7-fold (from 94/mm^2 to 33/mm^2), which was similar to the 4.4-fold decrease observed by Carreras *et al.* (from 9.6 to 2.2%). Furthermore, the proportional differences in the amount of FOXP3$^+$ cells in neoplastic follicles of FL and in normal GC from tonsils and lymph nodes were similar in the two studies. Our results cannot be compared to those of other publications on FL and DLBCL since the authors used a *hot-spot* quantification technique and did not detail their morphometric and case distribution data.[11,23,26] In cHL, some differences from the study by Alvaro *et al.* could also be related to the *hot-spot* technique.[9] Again, the relative proportion of cHL cases with FOXP3$^+$ cell counts over the mean±10%, as used by Alvaro *et al.*,[9] was similar to that in our study (20.4% and 19.2%, respectively).

Our study is the first to apply ROC curves for determination of cut-off levels.[37] Linking the results for the prognostic importance of FOXP3$^+$ cell quantity in the various lymphoma subtypes to overall, disease-specific and failure-free survival, allowed the identification of distinct entity-specific cut-off values for FOXP3$^+$ cell density for these clinical end-points. Analyzing the prognostic value of FOXP3$^+$ cell quantity in a differentiated manner, we suggest a positive prognostic influence of an increased amount of these cells not only in FL and cHL, but also, by factoring the probable tumor cell origin in DLBCL, in GC-like DLBCL defined by Hans' algorithm,[36] which would have been masked when

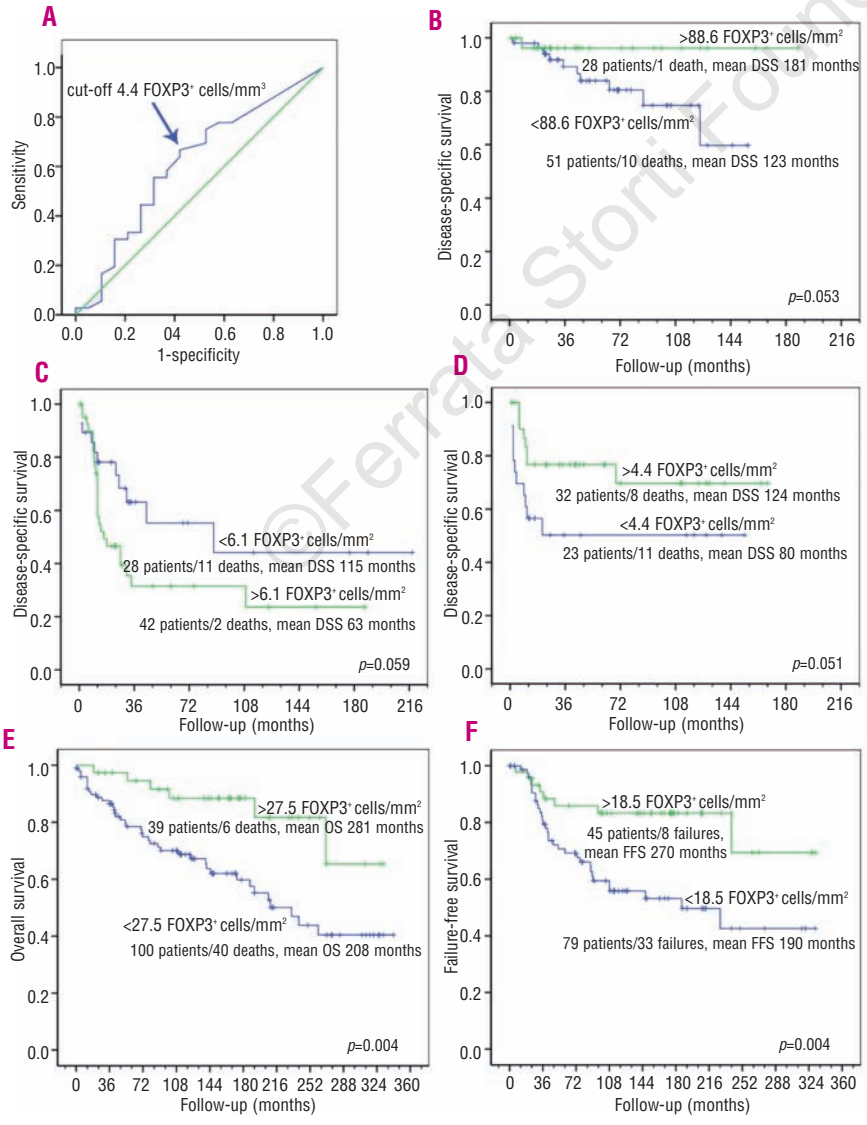

Figure 2. (A) Receiver operating characteristics (ROC)-curve indicating the prognostic discriminatory power of FOXP3$^+$ cells/mm^2 in germinal center-like diffuse large B-cell lymphomas. Note that the labeled curve point at a sensitivity of 0.67 (67%) and specificity of 0.58 (58%) (1-specificity =0.42) is closest to coordinates (0.0;1.0). Considering disease-specific survival, these coordinates correspond to an optimal cut-off for the amount of FOXP3$^+$ cells/mm^2 at 4.4 cells/mm^2. (B) Kaplan-Meier disease-specific survival analysis in follicular lymphomas with respect to numbers of FOXP3$^+$ cells/mm^2 and cut-offs calculated by ROC. (C) Kaplan-Meier disease-specific survival analysis in non-germinal center diffuse large B-cell lymphomas with respect to the number of FOXP3$^+$ cells/mm^2 and cut-offs calculated by ROC. (D) Kaplan-Meier disease-specific survival analysis in germinal center-like diffuse large B-cell lymphomas with respect to the number of FOXP3$^+$ cells/mm^2 and cut-offs calculated by ROC. (E) Kaplan-Meier overall survival analysis in classical Hodgkin's lymphomas with respect to the number of FOXP3$^+$ cells/mm^2 and cut-offs calculated by ROC. (F) Kaplan-Meier failure-free survival analysis in classical Hodgkin's lymphomas with respect to the number of FOXP3$^+$ cells/mm^2 and cut-offs calculated by ROC. *See also Table 3.*

©Ferrata Storti Foundation

Table 4. Multivariate analysis for the independent prognostic value of FOXP3+ cell density considering overall survival, disease-specific survival and failure-free survival in selected lymphoma entities.

Entity	*Factor*	*Relative risk (range)*	*p value*
GC-like DLBCL[DSS]	Age	1.03 (0.99-1.07)	0.134
	Stage	1.30 (0.82-2.06)	0.268
	FOXP3	0.39 (0.14-1.08)	0.079
Non-GC DLBCL[DSS]	Age	1.04 (1.01-1.07)	0.017
	Stage	1.57 (1.08-2.29)	0.019
	FOXP3	2.27 (0.93-5.55)	0.071
cHL, all[OS]	Age	1.06 (1.04-1.09)	<0.0001
	B-symptoms	1.56 (0.67-4.62)	0.302
	Stage	1.10 (0.71-1.69)	0.663
	FOXP3	0.43 (0.16-1.13)	0.087
cHL, mixed cellularity[OS]	Age	1.06 (1.02-1.10)	0.004
	B-symptoms	1.43 (0.24-8.55)	0.695
	Stage	1.54 (0.64-3.71)	0.338
	FOXP3	0.12 (0.02-1.03)	0.054
cHL, all[FFS]	Stage	1.4 (1.01-2.07)	0.047
	FOXP3	0.4 (0.19-0.89)	0.026
cHL, nodular sclerosis[FFS]	Stage	1.6 (1.05-2.59)	0.031
	FOXP3	0.2 (0.06-0.72)	0.013

Factors were selected on the basis of potential statistical significance in univariate models (p<0.1). OS, overall survival; DSS, disease-specific survival; FFS, failure-free survival

analyzing all DLBCL cases collectively.[26] Taken together, our findings and previous observations,[9-11,19-22] point towards the possibility of retained direct or indirect cellular communications between Treg and B-cell lymphoma cells in GC-associated neoplasms. Since we were not able to define any correlation between FOXP3+ cell numbers and lymphoma cell cycle deregulation, surface protein expression or Epstein-Barr virus, particularly in cHL, we suggest that the ability of FOXP3+ Treg to directly suppress and even kill B cells,[21,22] to suppress T_{FH} and T_{FH}-mediated B-cell functions such as survival,[19,21] and to allow the accumulation of large numbers of TIA-1+ cells,[9,26] could be important in GC-derived lymphomas. Interestingly, the observed trend towards better overall survival in AILT with increased FOXP3+ cell numbers also points to possible retained cellular communication loops between Treg and GC T_{FH}; the neoplastic cells of AILT being regarded as molecularly linked to T_{FH}.[41] Contrary to GC-like DLBCL, but similarly to epithelial malignancies, in non-GC DLBCL and Hans'-unclassifiable DLBCL (*data not shown*), increased FOXP3+ cell numbers correlated with an adverse clinical outcome (disease-specific and failure-free survival rates) despite the fact that the absolute FOXP3+ cell numbers were similar in GC-like and non-GC DLBCL. The reason for this phenomenon is unclear, but assuming that non-GC DLBCL are derived from activated B-cells from later developmental stages, the recently observed dysfunctional Treg in another late-developmental stage B-cell neoplasia, multiple myeloma, is intriguing.[42] In such post-GC derived B-cell neoplasms, there might be additional cell communication loops leading to functional down-regulation of Treg. Indeed, the cytokines interleukin-6 and tumor necrosis factor-α are differently distributed among GC and non-GC DLBCL with particularly high levels in non-GC DLBCL.[43] Both interleukin-6[44,45] and tumor necrosis factor-α[46] can inhibit the function of Treg, suggesting that an increased number of Treg, more frequently observed by us in non-GC DLBCL with adverse clinical outcomes, may not reflect their functional activity.

In summary, our standardized TMA-based morphometric approach and ROC-based analysis for determining cut-off levels revealed profound quantitative differences in FOXP3+ cell distribution among different lymphoma entities, provided further evidence that FOXP3+ cells probably represent important lymphoma/host microenvironment modulators in distinct lymphoproliferative diseases, and demonstrated that increased FOXP3+ cell numbers can positively influence survival in GC-derived neoplasms such as FL, GC-like DLBCL and cHL.

Authorship and Disclosures

AT designed the study, collected cases, constructed the TMA, performed, together with CM, the morphological analysis, performed the statistical analysis and wrote the manuscript; CM performed, together with AT, the morphological analysis and generated the statistical tables; PH performed the immunohistochemical stainings and double-stainings; PW collected cases, constructed TMA, contributed to writing the manuscript, and critically read the manuscript; SAP collected cases, contributed to writing the manuscript, and critically read the manuscript; SD supervised the work, contributed to writing the manuscript, substantially contributed to the discussion of the results, collected cases, and critically read the manuscript.

The authors reported no potential conflicts of interest.

©Ferrata Storti Foundation

References

1. Beyer M, Schultze JL. Regulatory T cells in cancer. Blood 2006;108:804-11.
2. Petrulio CA, Kim-Schulze S, Kaufman HL. The tumour microenvironment and implications for cancer immunotherapy. Expert Opin Biol Ther 2006;6:671-84.
3. Wei WZ, Morris GP, Kong YC. Anti-tumor immunity and autoimmunity: a balancing act of regulatory T cells. Cancer Immunol Immunother 2004; 53:73-8.
4. Hori S, Nomura T, Sakaguchi S. Control of regulatory T cell development by the transcription factor Foxp3. Science 2003;299:1057-61.
5. Fontenot JD, Rasmussen JP, Williams LM, Dooley JL, Farr AG, Rudensky AY. Regulatory T cell lineage specification by the forkhead transcription factor foxp3. Immunity 2005;22:329-41.
6. Gavin MA, Rasmussen JP, Fontenot JD, Vasta V, Manganiello VC, Beavo JA, et al. Foxp3-dependent programme of regulatory T-cell differentiation. Nature 2007;445:771-5.
7. Chai JG, Xue SA, Coe D, Addey C, Bartok I, Scott D, et al. Regulatory T cells, derived from naive $CD4^+CD25^-$ T cells by in vitro Foxp3 gene transfer, can induce transplantation tolerance. Transplantation 2005;79:1310-6.
8. Dave SS, Wright G, Tan B, Rosenwald A, Gascoyne RD, Chan WC, et al. Prediction of survival in follicular lym-

phoma based on molecular features of tumor-infiltrating immune cells. N Engl J Med 2004;351:2159-69.
9. Alvaro T, Lejeune M, Salvado MT, Bosch R, Garcia JF, Jaen J, et al. Outcome in Hodgkin's lymphoma can be predicted from the presence of accompanying cytotoxic and regulatory T cells. Clin Cancer Res 2005; 11:1467-73.
10. Carreras J, Lopez-Guillermo A, Fox BC, Colomo L, Martinez A, Roncador G, et al. High numbers of tumor-infiltrating FOXP3-positive regulatory T cells are associated with improved overall survival in follicular lymphoma. Blood 2006;108:2957-64.
11. Lee AM, Clear AJ, Calaminici M, Davies AJ, Jordan S, MacDougall F, et al. Number of CD4+ cells and location of forkhead box protein P3-positive cells in diagnostic follicular lymphoma tissue microarrays correlates with outcome. J Clin Oncol 2006;24: 5052-9.
12. de Jong D. Molecular pathogenesis of follicular lymphoma: a cross talk of genetic and immunologic factors. J Clin Oncol 2005;23:6358-63.
13. Tzankov A, Dirnhofer S. Pathobiology of classical Hodgkin lymphoma. Pathobiology 2006;73: 107-25.
14. Camacho SA, Kosco-Vilbois MH, Berek C. The dynamic structure of the germinal center. Immunol Today 1998;19:511-4.
15. Parker DC. T cell-dependent B cell activation. Annu Rev Immunol 1993;11:331-60.
16. Bouzahzah F, Bosseloir A, Heinen E, Simar LJ. Human germinal center CD4+CD57+ T cells act differently on B cells than do classical T-helper cells. Dev Immunol 1995;4:189-97.
17. Andersson E, Dahlenborg K, Ohlin M, Borrebaeck CA, Carlsson R. Immunoglobulin production induced by CD57+ GC-derived helper T cells in vitro requires addition of exogenous IL-2. Cell Immunol 1996;169: 166-73.
18. Rasheed AU, Rahn HP, Sallusto F, Lipp M, Muller G. Follicular B helper T cell activity is confined to CXCR5(hi)ICOS(hi) CD4 T cells and is independent of CD57 expression. Eur J Immunol 2006;36:1892-903.
19. Lim HW, Hillsamer P, Kim CH. Regulatory T cells can migrate to follicles upon T cell activation and suppress GC-Th cells and GC-Th cell-driven B cell responses. J Clin Invest 2004;114:1640-9.
20. Marinova E, Han S, Zheng B. Germinal center helper T cells are dual functional regulatory cells with suppressive activity to conventional CD4+ T cells. J Immunol 2007;178: 5010-7.
21. Lim HW, Hillsamer P, Banham AH, Kim CH. Cutting edge: direct suppression of B cells by CD4+ CD25+ regulatory T cells. J Immunol 2005; 175:4180-3.
22. Zhao DM, Thornton AM, DiPaolo RJ, Shevach EM. Activated CD4+CD25+ T cells selectively kill B lymphocytes. Blood 2006;107:3925-32.
23. Alvaro T, Lejeune M, Salvado MT, Lopez C, Jaen J, Bosch R, et al. Immunohistochemical patterns of reactive microenvironment are associated with clinicobiologic behavior in follicular lymphoma patients. J Clin Oncol 2006;24:5350-7.
24. Marshall NA, Christie LE, Munro LR, Culligan DJ, Johnston PW, Barker RN, et al. Immunosuppressive regulatory T cells are abundant in the reactive lymphocytes of Hodgkin lymphoma. Blood 2004;103:1755-62.
25. Yang ZZ, Novak AJ, Stenson MJ, Witzig TE, Ansell SM. Intratumoral CD4+CD25+ regulatory T-cell-mediated suppression of infiltrating CD4+ T cells in B-cell non-Hodgkin lymphoma. Blood 2006;107:3639-46.
26. Hasselblom S, Sigurdadottir M, Hansson U, Nilsson-Ehle H, Ridell B, Andersson PO. The number of tumour-infiltrating TIA-1+ cytotoxic T cells but not FOXP3+ regulatory T cells predicts outcome in diffuse large B-cell lymphoma. Br J Haematol 2007;137:364-73.
27. Klemke CD, Fritzsching B, Franz B, Kleinmann EV, Oberle N, Poenitz N, et al. Paucity of FOXP3+ cells in skin and peripheral blood distinguishes Sezary syndrome from other cutaneous T-cell lymphomas. Leukemia 2006;20:1123-9.
28. Jaffe ES, Harris NL, Stein H, Vardiman JW, eds. Pathology and Genetics of Tumours of Haematopoietic and Lymphoid Tissues. Lyon: IARC Press. 2001.
29. Tzankov A, Pehrs AC, Zimpfer A, Ascani S, Lugli A, Pileri S, et al. Prognostic significance of CD44 expression in diffuse large B cell lymphoma of activated and germinal centre B cell-like types: a tissue microarray analysis of 90 cases. J Clin Pathol 2003; 56:747-52.
30. Tzankov A, Went P, Zimpfer A, Dirnhofer S. Tissue microarray technology: principles, pitfalls and perspectives—lessons learned from hematological malignancies. Exp Gerontol 2005;40:737-44.
31. Tzankov A, Gschwendtner A, Augustin F, Fiegl M, Obermann EC, Dirnhofer S, et al. Diffuse large B-cell lymphoma with overexpression of cyclin E substantiates poor standard treatment response and inferior outcome. Clin Cancer Res 2006;12:2125-32.
32. Tzankov A, Heiss S, Ebner S, Sterlacci W, Schaefer G, Augustin F, et al. Angiogenesis in nodal B-cell lymphomas: a high throughput study. J Clin Pathol 2007;60:476-82.
33. Tzankov A, Went P, Münst S, Papadopoulos T, Jundt G, Dirnhofer S. Rare expression of BSAP (PAX-5) in mature T-cell lymphomas. Mod Pathol 2007;20:632-7.
34. Zimpfer A, Bernasconi B, Glatz K, Lugli A, Krugmann J, Fend F, et al. Trisomy 3 and gain of an X-chromosome are frequent genetic abnormalities in gastric B-cell lymphomas. Analysis by FISH on tissue microarrays of 226 surgically resected cases. J Clin Pathol 2002;55 [Suppl 1]:A20.
35. Zimpfer A, Went P, Tzankov A, Pehrs AC, Lugli A, Maurer R, et al. Rare expression of KIT (CD117) in lymphomas: a tissue microarray study of 1166 cases. Histopathology 2004; 45:398-404.
36. Hans CP, Weisenburger DD, Greiner TC, Gascoyne RD, Delabie J, Ott G, et al. Confirmation of the molecular classification of diffuse large B-cell lymphoma by immunohistochemistry using a tissue microarray. Blood 2004;103:275-82.
37. Perkins NJ, Schisterman EF. The inconsistency of "optimal" cutpoints obtained using two criteria based on the receiver operating characteristic curve. Am J Epidemiol 2006;163: 670-5.
38. Kasprzycka M, Marzec M, Liu X, Zhang Q, Wasik MA. Nucleophosmin/anaplastic lymphoma kinase (NPM/ALK) oncoprotein induces the T regulatory cell phenotype by activating STAT3. Proc Natl Acad Sci USA 2006;103:9964-9.
39. Mitterlechner T, Fiegl M, Mühlbock H, Oberaigner W, Dirnhofer S, Tzankov A. Epidemiology of non-Hodgkin lymphomas in Tyrol/Austria from 1991 to 2000. J Clin Pathol 2006;59:48-55.
40. Roncador G, Brown PJ, Maestre L, Hue S, Martinez-Torrecuadrada JL, Ling KL, et al. Analysis of FOXP3 protein expression in human CD4+CD25+ regulatory T cells at the single-cell level. Eur J Immunol 2005;35:1681-91.
41. de Leval L, Rickman DS, Thielen C, de Reynies A, Huang YL, Delsol G, et al. The gene expression profile of nodal peripheral T-cell lymphoma demonstrates a molecular link between angioimmunoblastic T-cell lymphoma (AITL) and follicular helper T cells (TFH). Blood 2007; 109:4952-63.
42. Prabhala RH, Neri P, Bae JE, Tassone P, Shammas MA, Allam CK, et al. Dysfunctional T regulatory cells in multiple myeloma. Blood 2006; 107:301-4.
43. Pedersen LM, Jurgensen GW, Johnsen HE. Serum levels of inflammatory cytokines at diagnosis correlate to the bcl-6 and CD10 defined germinal centre (GC) phenotype and bcl-2 expression in patients with diffuse large B-cell lymphoma. Br J Haematol 2005; 128:813-9.
44. Doganci A, Eigenbrod T, Krug N, De Sanctis GT, Hausding M, Erpenbeck VJ, et al. The IL-6R α chain controls lung CD4+CD25+ Treg development and function during allergic airway inflammation in vivo. J Clin Invest 2005;115:313-25.
45. Wan S, Xia C, Morel L. IL-6 produced by dendritic cells from lupus-prone mice inhibits CD4+CD25+ T cell regulatory functions. J Immunol 2007; 178:271-9.
46. Valencia X, Stephens G, Goldbach-Mansky R, Wilson M, Shevach EM, Lipsky PE. TNF downmodulates the function of human CD4+CD25hi T-regulatory cells. Blood 2006;108:253-61.

©Ferrata Storti Foundation